American Mineralogist, Volume 76, pages 161–175, 1991

Ferric iron in metamorphic biotite and its petrologic and crystallochemical implications

Charles V. Guidotti
Department of Geological Sciences, University of Maine at Orono, Orono, Maine 04469, U.S.A.
M. Darby Dyar
Department of Geological Sciences, University of Oregon, Eugene, Oregon 97403, U.S.A.

Abstract

Mössbauer spectroscopy data for the Fe^{3+} contents of biotite from metapelitic rocks of northwestern Maine was accumulated in the context of metamorphic grade for Al-, Si-, and Ti-saturated limiting assemblages. Specimens from two areas contain graphite; those from a third area, magnetite.

The results show: (1) all biotites have 8 ± 3% of Fe_{tot} as $^{[4]}Fe^{3+}$; (2) biotite coexisting with graphite contains only 4% of Fe_{tot} as $^{[6]}Fe^{3+}$, whereas those coexisting with magnetite contain significant $^{[6]}Fe^{3+}$ (10–13% of Fe_{tot}); (3) Fe^{3+} contents are independent of metamorphic grade and silicate mineral assemblage; and (4) partitioning of Fe^{2+} into M2 vs. M1 is ca. $^3/_1$, not the expected $^2/_1$, and is independent of T. Whether Fe^{2+} is ordering directly or in response to the ordering of other cations is ambiguous.

The new Fe^{2+} data, plus discussions in the literature suggesting the possibility that interlayer site deficiencies involve replacement of alkalis by H_3O^+, taken in conjunction with petrologic constraints, support the basis for some site substitution models for biotite. Two such substitutions are: K^+, $Na^+ \rightleftharpoons H_3O^+$ and Ti^{4+} + octahedral vacancies $\rightleftharpoons 2(R^{2+})$.

Data now available for biotite from graphite-bearing rocks suggest a need for modification of biotite activity models. The data also imply some nonideal aspects of biotite substitutions.

It remains unclear if the Fe^{3+} content typical of biotite from graphite-bearing rocks significantly affects application of the various garnet-biotite geothermometers. However, the Fe^{3+} content typical of biotite from magnetite-bearing rocks must be considered if one expects reasonable results from garnet-biotite geothermometry.

Introduction

Many mineralogic and petrologic studies are plagued by imperfect characterization of minerals. Included are the problems of Fe^{2+} and Fe^{3+} and the number of O atoms present in a formula unit. Commonly, analytical constraints force the assumption that all Fe is Fe^{2+} and that formulas have a fixed number of O atoms.

Such simplifications are approximations. To the extent that minerals deviate therefrom, problems arise in formulating solution and activity models, thereby affecting studies on geothermometry, geobarometry, and the calculation of fluid compositions present during petrologic processes. Determination of site substitutions also suffers from imperfect characterization of minerals.

This report focuses on the Fe^{3+} content of biotite from metapelites formed over a range of metamorphic grades and coexisting with either graphite or magnetite. The amount and site occupancy of Fe^{3+} are considered in terms of both crystallochemical and petrologic factors. This presentation is part of ongoing work now being expanded to other phases in metapelites formed over a range of metamorphic grades and at different levels of oxidation.

Structural aspects of biotite relevant to this study have been reviewed by Bailey (1984). For our purposes, biotite is structurally a simple trioctahedral mica with only minor deviations toward a dioctahedral structure. In metamorphic biotite (Guidotti, 1984) the tetrahedral sites are often considered to contain only Si and Al, whereas the octahedral sites contain mainly Fe^{2+} and Mg with lesser, but still significant amounts of Al. Other octahedral cations commonly present in minor amounts include Ti^{4+}, Fe^{3+}, and Mn^{2+}. Two different types of octahedral positions are distinguished in the trioctahedral sheet, M1 and M2. M1 lies on the mirror plane in the 1M structure. X-ray structure studies show no evidence for either Si-Al ordering in the tetrahedral sites or Mg-Fe ordering between the M1 and M2 octahedral sites. The Mössbauer data presented in this study provide further insights on this latter point, as well as the amount of Fe^{3+} present and its site allocation.

Petrologic framework

Most biotite samples are from Areas A and B of Figure 1 in western Maine. Both areas are underlain mainly by

0003–004X/91/0102–0161$02.00

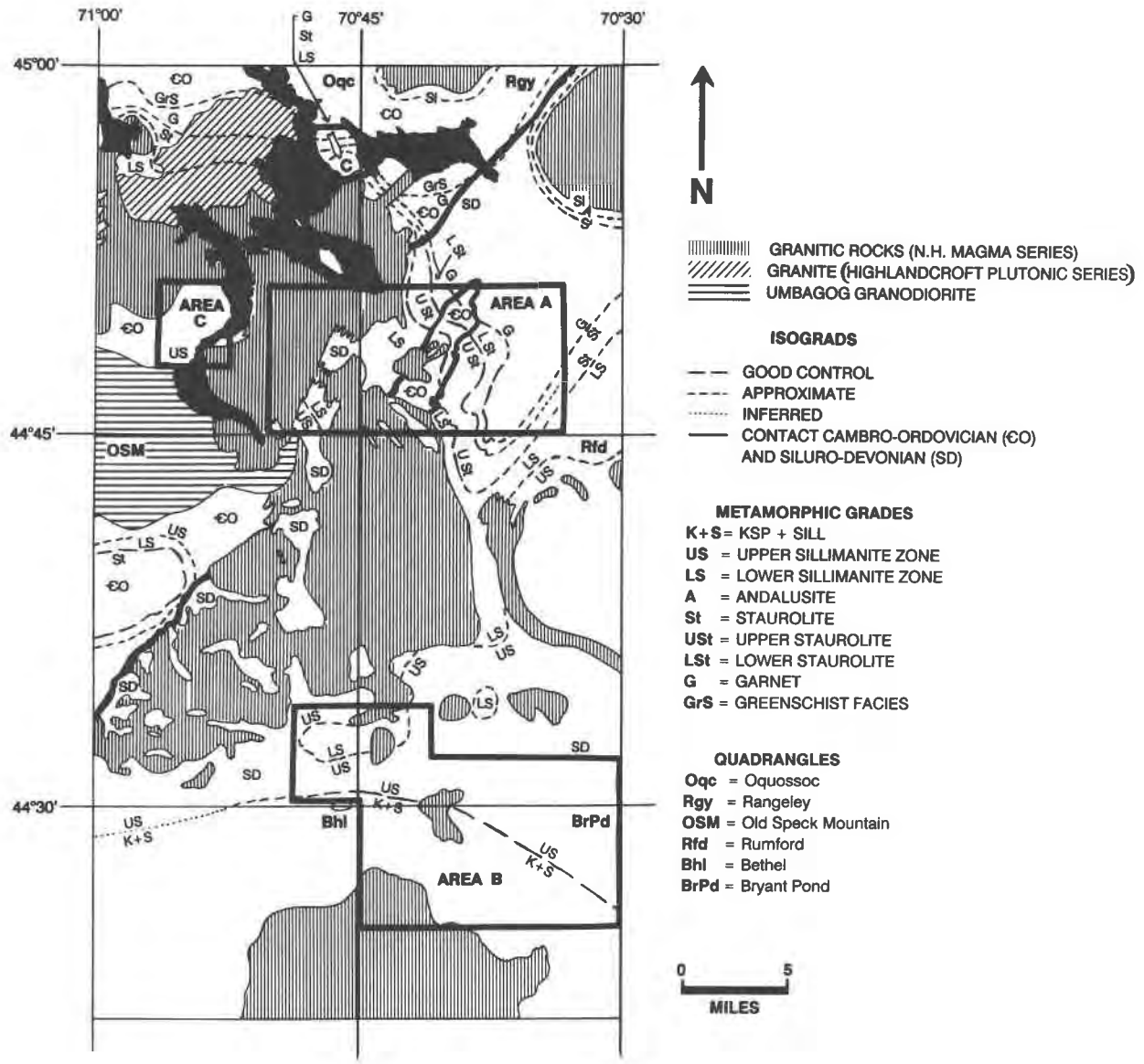

Fig. 1. Location of Areas A, B, and C in western Maine. Geology is generalized from Osberg et al. (1985).

Siluro-Devonian strata (Osberg et al., 1985). Detailed lists of assemblages are in Table 1. Petrologic and mineralogic studies covering Area A including Guidotti (1970a, 1970b, 1973, 1974, and 1978) and Foster (1977). Recently, Guidotti et al. (1988) discussed the compositional aspects of biotite in this area and that report provides a framework for this study. Figure 2 shows the distribution of metamorphic grades and AFM diagrams for Area A.

Biotite from Area A considered here is mainly from the limiting assemblages designated with a star on the AFM diagrams in Figure 2. All coexist with muscovite, quartz, and ilmenite and almost all with graphite. These restrictions ensure that biotite composition will be Al, Si, and Ti saturated, and controlled only by metamorphic grade [see Guidotti et al. (1988) for specific equilibria]. The presence of graphite and ilmenite containing less than 2.5 mol% hematite (Henry, 1981) ensures an f_{O_2} uniformly near the low range of possible values in metapelites. Hence, the amount of Fe^{3+} in the biotite represents the minimum amount likely to be present in samples from metapelites.

Samples from Area B (Fig. 1) are mineralogically identical to those from Area A but some experienced higher grade metamorphism (into the potassium feldspar + sillimanite zone, Table 1). Mineralogical and petrological studies on Area B include Guidotti (1963), Evans and Guidotti (1966), Guidotti et al. (1973), Cheney (1975), and Cheney and Guidotti (1979). For both Areas A and B, the studies strongly indicate that the mineral assemblages closely approach chemical equilibrium.

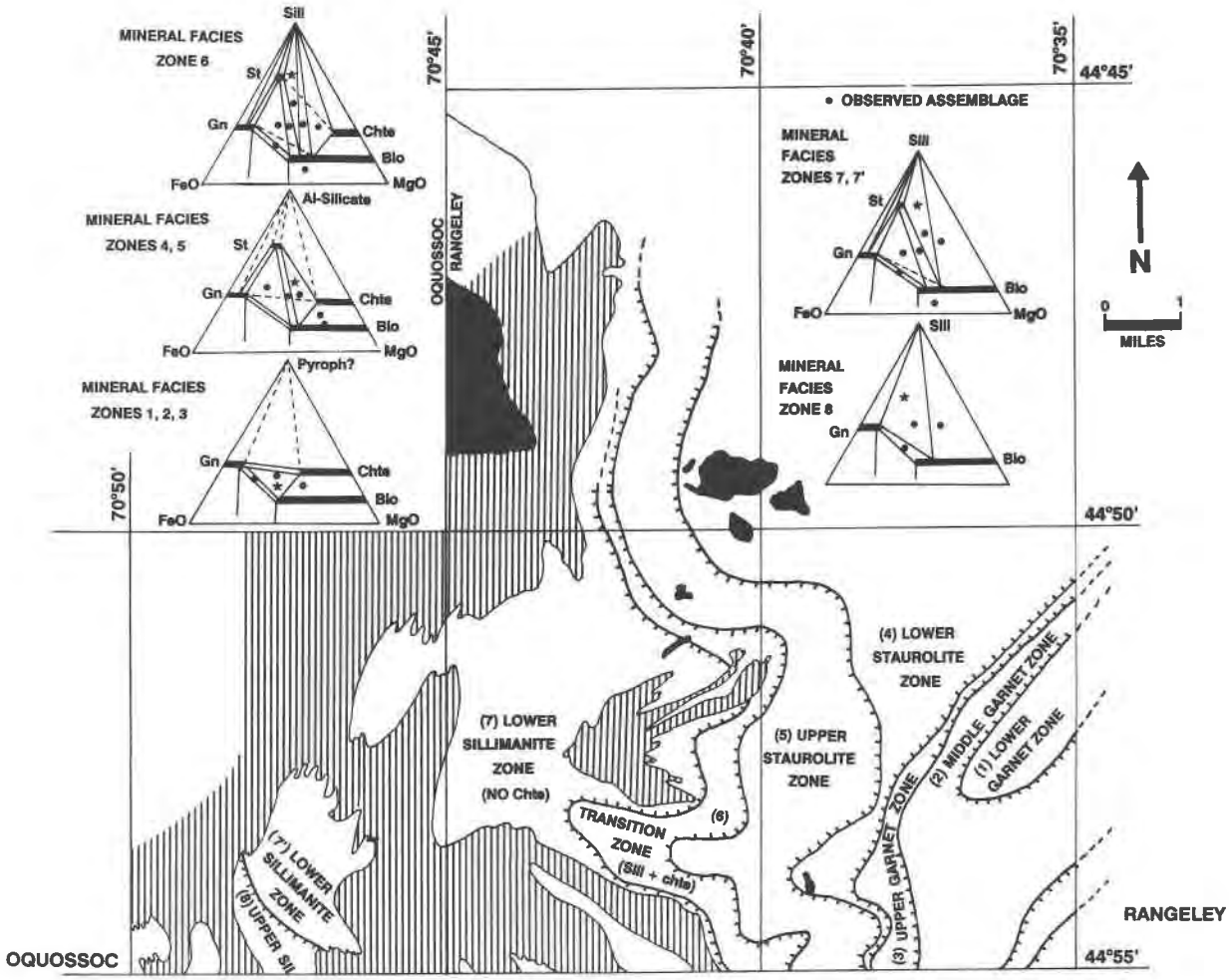

Fig. 2. Distribution of metamorphic grades and mineral facies diagrams for Area A. (Based upon Guidotti et al., 1988). Assemblages designated by a star are the limiting assemblages considered in this study. Muscovite + quartz are found in all assemblages shown.

Area C (Fig. 1) involves Cambro-Ordovician strata. Its metamorphism has been only briefly discussed in Green and Guidotti (1968), Guidotti (1970a), and Guidotti (1977). However, detailed studies by Green (1963), and Al-Mishwt (1972) in the areas to the west and northwest, respectively, of Area C have direct relevance to the petrology of Area C.

The mineral assemblages, range of bulk composition, and metamorphic grades of Area C are similar to those in the higher grades of Area A, although a later, low-grade event may have offset the earlier high temperature equilibria. Indeed, the isograd maps shown by Guidotti (1970a), Green and Guidotti (1968), Holdaway et al. (1982), and Guidotti (1985) show continuity of isograds between Areas A and C. The main difference of Area C relative to Areas A and B is the occurrence of magnetite in the metapelites.

Table 2 gives the average biotite analysis in each grade of Areas A and B, and in two sets of samples from Area C. The numbers shown represent recalculations of the average analyses to reflect the average Fe^{3+} content and site occupancy data provided by the Mössbauer study for each grade (see Table 3 and later discussion). Individual biotite analyses were considered elsewhere (Cheney, 1975; Guidotti et al., 1988; and Dyar, 1990).

For biotite samples from Areas A and B the main chemical variations relevant to this study are given in Table 4. Concomitant with these chemical changes the biotite changes pleochroic color from light orange brown to reddish brown. This change is in reponse to the increase of Ti as discussed by Guidotti (1984). It is related to a charge-transfer effect resulting from Fe^{2+}-Ti^{4+} interaction (Faye, 1968).

Also considered from Area A (but excluded from the averages given in Tables 2 and 4) are a few biotite samples from sillimanite zone, nonlimiting assemblages (O-

TABLE 1. Summary of petrologic data on biotite studied by Mössbauer spectroscopy

Sample name	Area	Zone no.	Zone name	Ilm	Rt	Po	Gr	Remarks
Ra-d75-66	A	1	Lower garnet, Rangeley	X	0	?	X	
Ra-d72-66	A	1	Lower garnet, Rangeley	X	0	0	0	
Ra-d9-66	A	2	Middle garnet, Rangeley	X	0	0	0	
Ra-d28-66	A	2	Middle garnet, Rangeley	X	0	?	0	
Ra-c95-66	A	2	Middle garnet, Rangeley	X	0	0	0	
Ra-d86-66	A	2	Middle garnet, Rangeley	X	0	0	X	
Ra-d11-66	A	3	Upper garnet, Rangeley	X	0	0	X	
Ra-d37-66	A	3	Upper garnet, Rangeley	X	0	X	X	
Ra-d12-66	A	3	Upper garnet, Rangeley	X	0	0	X	
Ra-d14-66	A	3	Upper garnet, Rangeley	X	0	0	X	
Ra-d60-66	A	4	Lower staur., Rangeley	X	0	X	X	
Ra-a65-66	A	4	Lower staur., Rangeley	X	0	X	X	
Ra-c1-66	A	4	Lower staur., Rangeley	X	0	0	X	
Ra-c4-66	A	4	Lower staur., Rangeley	X	0	X	X	
Ra-a73-66	A	5	Upper staur., Rangeley	X	0	X	X	
Ra-a14-66	A	5	Upper staur., Rangeley	X	0	X	X	
Ra-a69-66	A	5	Upper staur., Rangeley	X	0	0	X	
Ra-a33-66	A	5	Upper staur., Rangeley	X	0	0	X	
Ra-b53-66	A	6	Transition zone, Rangeley	X	0	?	X	
Ra-b48-66	A	6	Transition zone, Rangeley	X	0	?	X	
Ra-a57-66	A	6	Transition zone, Rangeley	X	0	X	X	
Ra-a96-66	A	6	Transition zone, Rangeley	X	0	X	X	
Ra-a93-66	A	6	Transition zone, Rangeley	X	0	0	X	
Ra-b4-66	A	7	Lower sill., Rangeley	X	0	X	X	
Ra-b41-66	A	7	Lower sill., Rangeley	X	0	X	?	
Ra-a95-66	A	7	Lower sill., Rangeley	X	0	X	X	
O-K-53	A	7′	Lower sill., Oquossoc	X	0	X	X	
O-K-15	A	7′	Lower sill., Oquossoc	X	0	X	X	
O-L-10	A	7′	Lower sill., Oquossoc	X	0	0	?	
O-J-65	A	7′	Lower sill., Oquossoc	X	0	0	X	
O-K-8′	A	8*	Upper sill., Oquossoc	0	X	X	?	Sulfide-rich
O-K-8	A	8*	Upper sill., Oquossoc	0	X	X	?	Sulfide-rich
O-K-9	A	8*	Upper sill., Oquossoc	0	X	X	X	Sulfide-rich
O-C-30	A	8	Upper sill., Oquossoc	X	0	X	X	
O-C-26	A	8	Upper sill., Oquossoc	X	0	0	X	
O-C-14	A	8	Upper sill., Oquossoc	X	0	X	?	
O-C-18	A	8	Upper sill., Oquossoc	X	0	0	X	
O-K-10	A	8	Upper sill., Oquossoc	X	0	0	?	
9-8/7/63	B	8′	Upper sill., Bryant Pond	X	0	X	X	
16-8/23/60	B	8′	Upper sill., Bryant Pond	X	0	0	X	
4-7/26/59	B	8′	Upper sill., Bryant Pond	X	0	0	X	
16-7/18/60	B	9	Kfs + sill., Bryant Pond	0	0	X	0	
15-8/18/59	B	9	Kfs + sill., Bryant Pond	X	0	X	X	Po fairly abundant
14-7/2/60	B	9	Kfs + sill., Bryant Pond	X	0	0	X	
5-9/20/61	B	9	Kfs + sill., Bryant Pond	X	0	0	X	
O-b-41	A	—	Granite (Oquossoc)	X	0	0	0	Granite
O-I-1	C	—	Staur., Oquossoc	X	0	X	0	Magnetite
O-G-92	C	—	And. + staur., Oquossoc	X	0	0	0	Magnetite
O-H-49′	C	—	Upper sill., Oquossoc	X	0	X	0	Magnetite
O-H-56	C	—	Upper sill., Oquossoc	X	0	0	0	Magnetite
O-H-72	C	—	Upper sill., Oquossoc	X	0	0	0	Magnetite
O-B-16	C	—	Staur., Oquossoc	X	0	0	0	Magnetite, hematite

Note: Ilm = ilmenite, Rt = rutile, Po = pyrrhotite, Gr = graphite, X = Present, ? = Probably present, 0 = Not present. For Area A the zone nos. are keyed to assemblages designated with a star on Figure 2, excluding * samples.

* Sulfide-rich samples not included in averages in Tables 2 and 4.

K-8, etc.) in which the rocks contain abundant sulfide (pyrrhotite, ca. 6%). These rocks show the effects of sulfidation reactions (Guidotti et al., 1977a, 1977b, 1988). Thus the $Mg/(Mg + Fe^{2+})$ ratio of the biotite is in the range of 0.65–0.74, the Ti content is only 0.233, Fe-rich minerals like garnet and staurolite are absent, and rutile takes the place of ilmenite as the Ti oxide phase.

Area C biotite samples are from limiting assemblages such as Sil + St + Bt + Grt and Sil + Bt + Grt, etc. (abbreviations following Kretz, 1983). The main petrographic difference in biotite samples from Area C relative to those from Areas A and B is the pleochroism. Biotite samples from Area C exhibit colors in various shades of dark greenish brown.

METHODS AND RESULTS

The 52 biotite samples used in this study were analyzed for major elements by electron microprobe analyses at the University of Wisconsin at Madison and the Smithsonian Astrophysical Observatory in Cambridge, Massachusetts. At both locations an acceleration potential of 15 keV was used with sample currents ranging from 10 to 40 nA. Natural and synthetic minerals were used as standards for major elements, whereas synthetic glasses

TABLE 2. Average chemical compositions of biotite

Area	A	A	A	A	A	A	A	A	A	A	A	A	A	A	B
Zone	Lower garnet		Middle garnet		Upper garnet		Lower staurolite		Upper staurolite		Tansition zone		Lower sillimanite		
Zone no.	1	1	2	2	3	3	4	4	5	5	6	6	7	7	7
Analyses	T.S.	G.	T.S.	G.	T.S.	G.	T.S.	G.	T.S.	G.	T.S.	G.	T.S.	G.	C.
No. samples	2	13	4	16	4	13	4	8	4	15	5	18	3	10	3
SiO_2	35.14	35.42	35.23	35.62	36.09	35.56	35.56	35.52	35.82	35.81	36.01	35.95	35.69	35.62	35.83
Al_2O_3	19.56	19.50	19.68	19.79	19.90	20.02	19.73	19.84	20.07	19.99	19.89	19.90	20.25	20.16	19.56
FeO	19.82	19.36	20.09	19.92	17.67	17.95	17.96	17.87	17.39	17.34	17.37	17.22	19.05	18.71	18.11
Fe_2O_3	3.44	3.36	2.90	2.88	3.80	3.86	2.92	2.91	2.21	2.19	2.39	2.37	1.27	1.26	1.22
MgO	7.39	7.83	7.64	7.65	8.87	8.36	9.17	9.42	9.78	9.75	9.53	9.57	9.44	9.48	9.86
TiO_2	1.64	1.70	1.65	1.66	1.54	1.57	1.55	1.52	1.48	1.51	1.61	1.66	1.82	1.73	1.75
MnO	0.17	0.17	0.12	0.12	0.11	0.07	0.08	0.07	0.07	0.07	0.07	0.07	0.05	0.07	0.07
ZnO	0.06	0.04	0.04	0.06	0.07	0.06	0.04	0.01	0.11	0.01	0.07	0.03	0.04	0.06	8.27
K_2O	8.06	7.94	8.21	7.98	7.91	8.10	8.27	8.15	8.28	8.38	8.27	8.41	8.26	8.38	0.26
BaO	0.00	0.05	0.02	0.02	0.03	0.03	0.00	0.03	0.00	0.10	0.03	0.06	0.08	0.06	0.10
Na_2O	0.15	0.13	0.16	0.25	0.26	0.18	0.26	0.29	0.32	0.30	0.31	0.30	0.27	0.27	0.00
H_2O	3.93	3.95	3.94	3.97	4.02	3.98	3.98	3.99	4.00	3.99	4.00	4.00	4.01	3.99	3.97
Total	99.36	99.45	99.68	99.92	100.27	99.74	99.74	99.62	99.53	99.44	99.55	99.54	99.54	99.79	99.00
Si	5.358	5.377	5.355	5.385	5.386	5.352	5.361	5.344	5.372	5.378	5.399	5.392	5.342	5.352	5.410
$^{[4]}Al$	2.364	2.353	2.462	2.435	2.351	2.378	2.411	2.430	2.452	2.447	2.410	2.419	2.515	2.506	2.451
$^{[4]}Fe^{3+}$	0.278	0.270	0.183	0.180	0.263	0.270	0.228	0.226	0.176	0.175	0.191	0.189	0.143	0.142	0.139
$^{[4]}Sum$	8.000	8.000	8.000	8.000	8.000	8.000	8.000	8.000	8.000	8.000	8.000	8.000	8.000	8.000	8.000
$^{[6]}Al$	1.151	1.136	1.064	1.091	1.149	1.174	1.094	1.088	1.095	1.092	1.105	1.099	1.057	1.064	1.030
Fe^{2+}	2.528	2.458	2.554	2.519	2.205	2.260	2.264	2.248	2.181	2.178	2.178	2.160	2.385	2.351	2.287
$^{[6]}Fe^{3+}$	0.117	0.114	0.149	0.148	0.164	0.167	0.103	0.103	0.073	0.073	0.079	0.078	0.000	0.000	0.000
Mg	1.680	1.772	1.731	1.724	1.973	1.876	2.060	2.112	2.186	2.183	2.130	2.139	2.106	2.123	2.219
Ti	0.188	0.194	0.189	0.189	0.173	0.178	0.176	0.172	0.167	0.171	0.182	0.187	0.205	0.195	0.199
Mn	0.022	0.022	0.015	0.015	0.014	0.009	0.010	0.009	0.009	0.009	0.009	0.009	0.006	0.009	0.009
Zn	0.007	0.004	0.004	0.007	0.008	0.007	0.004	0.001	0.012	0.001	0.008	0.003	0.004	0.007	—
$^{[6]}Sum$	5.693	5.700	5.706	5.693	5.686	5.671	5.711	5.733	5.723	5.707	5.691	5.675	5.763	5.749	5.744
K	1.568	1.538	1.592	1.539	1.506	1.555	1.590	1.564	1.584	1.606	1.582	1.609	1.577	1.606	1.593
Na	0.044	0.038	0.047	0.073	0.075	0.053	0.076	0.085	0.093	0.087	0.090	0.087	0.078	0.079	0.076
Ba	0.000	0.003	0.001	0.001	0.002	0.002	0.000	0.002	0.000	0.006	0.002	0.004	0.005	0.004	0.006
$^{[12]}Sum$	1.612	1.579	1.640	1.613	1.583	1.610	1.666	1.651	1.677	1.699	1.680	1.700	1.660	1.689	1.675
Total	15.305	15.279	15.340	15.306	15.269	15.281	15.377	15.384	15.400	15.406	15.371	15.375	15.423	15.438	15.419

Area	A	A	B	A	A	B	B	B	B	B	C	C
Zone	Lower sillimanite			Upper sillimanite			Upper sillaminate		Ksp + sillimanite		Mt-bearing	Hm-bearing
Zone no.	7′	7′	7′	8	8	8	8′	8′	9	9	—	—
Analyses	T.S.	G.	C.	T.S.	G.	C.	T.S.	C.	T.S.	C.	T.S.	T.S.
No. samples	4	15	5	5	10	6	3	13	4	1	5	1
SiO_2	35.44	35.44	35.49	35.28	35.37	35.39	35.79	35.33	35.06	34.91	35.69	36.74
Al_2O_3	19.88	19.83	19.87	19.63	19.68	19.57	18.58	19.43	19.37	19.40	19.34	19.18
FeO	19.49	19.35	18.06	18.83	18.87	18.05	17.72	18.05	16.81	18.41	14.84	7.45
Fe_2O_3	2.28	2.26	2.11	2.39	2.38	2.28	2.47	2.28	2.47	2.71	4.78	7.05
MgO	8.07	8.14	9.14	8.07	8.21	8.86	8.36	8.86	8.03	8.82	9.68	12.91
TiO_2	1.82	1.88	1.75	2.47	2.31	2.12	2.12	2.12	3.21	2.74	1.83	1.32
MnO	0.13	0.10	0.09	0.15	0.15	0.13	0.13	0.13	0.22	0.18	0.23	0.23
ZnO	0.07	0.02	8.08	0.11	0.01	8.41	0.00	8.41	0.02	9.01	0.06	0.10
K_2O	8.39	8.49	0.25	8.75	8.76	0.25	8.63	0.25	9.17	0.23	9.02	7.34
BaO	0.02	0.08	0.10	0.00	0.11	0.13	0.00	0.13	0.04	0.00	0.14	0.18
Na_2O	0.26	0.26	0.00	0.25	0.23	0.00	0.29	0.00	0.15	0.00	0.20	0.05
H_2O	3.96	3.96	3.96	3.97	3.97	3.96	3.91	3.95	3.93	3.98	4.00	4.03
Total	99.81	99.81	98.90	99.93	100.05	99.15	98.00	98.94	98.48	100.39	99.81	96.58
Si	5.361	5.361	5.371	5.335	5.341	5.362	5.484	5.366	5.348	5.262	5.349	5.463
$^{[4]}Al$	2.516	2.517	2.515	2.484	2.479	2.465	2.302	2.438	2.430	2.499	2.430	2.434
$^{[4]}Fe^{3+}$	0.123	0.122	0.114	0.181	0.180	0.173	0.214	0.196	0.222	0.239	0.221	0.103
$^{[4]}Sum$	8.000	8.000	8.000	8.000	8.000	8.000	8.000	8.000	8.000	8.000	8.000	8.000
$^{[6]}Al$	1.028	1.019	1.029	1.015	1.023	1.029	1.053	1.040	1.053	0.947	0.986	0.927
Fe^{2+}	2.466	2.448	2.286	2.381	2.383	2.287	2.271	2.293	2.145	2.321	1.860	0.926
$^{[6]}Fe^{3+}$	0.137	0.135	0.126	0.091	0.090	0.087	0.071	0.065	0.062	0.068	0.318	0.686
Mg	1.820	1.835	2.062	1.819	1.848	2.001	1.909	2.006	1.826	1.981	2.162	2.861
Ti	0.207	0.214	0.199	0.281	0.262	0.242	0.244	0.242	0.368	0.311	0.206	0.148
Mn	0.017	0.013	0.012	0.019	0.019	0.017	0.017	0.017	0.028	0.023	0.029	0.029
Zn	0.008	0.002	—	0.012	0.001	—	0.000	—	0.002	—	0.007	0.001
$^{[6]}Sum$	5.683	5.666	5.744	5.618	5.626	5.663	5.562	5.663	5.484	5.651	5.568	5.588
K	1.619	1.638	1.560	1.688	1.687	1.625	1.687	1.630	1.785	1.732	1.724	1.392
Na	0.076	0.076	0.073	0.073	0.067	0.073	0.086	0.074	0.044	0.067	0.058	0.052
Ba	0.001	0.005	0.006	0.000	0.007	0.008	0.000	0.008	0.002	0.000	0.008	0.003
$^{[12]}Sum$	1.696	1.719	1.639	1.761	1.761	1.706	1.773	1.712	1.831	1.799	1.790	1.447
Total	15.379	15.385	15.383	15.379	15.387	15.369	15.335	15.375	15.315	14.900	15.358	15.035

Note: T.S. = samples in this study; G. = larger population of sample (Guidotti et al., 1988); C. = Bryant Pond Quadrangle samples (Cheney, 1975). The averages obtained from those studies have been adjusted to reflect average Fe^{3+} data presented in this report for the given metamorphic grade.

Table 3. Site occupancies of Fe atoms (% of total Fe)

Sample	Zone	$^{[4]}Fe^{3+}$	Fe^{3+} M1	Fe^{3+} M2	Fe^{2+} M1	Fe^{2+} M2	$\%Fe^{3+}$ total	Fe^{2+} M2:M1
Ra-d75-66	1	10	4	—	23	62	14	2.70
Ra-d72-66	1	9	4	—	19	68	13	3.58
Ra-d9-66	2	7	5	—	22	65	12	2.95
Ra-d28-66	2	9	—	5	21	67	14	3.19
Ra-c95-66	2	4	2	2	31	60	8	1.94
Ra-d86-66	2	6	6	—	24	64	12	2.66
Ra-d11-66	3	12	7	—	30	50	19	1.68
Ra-d37-66	3	6	4	7	21	62	17	2.95
Ra-d12-66	3	11	5	—	20	63	16	3.13
Ra-a14-66	3	11	2	—	22	64	13	2.90
Ra-d60-66	4	8	6	—	17	69	14	4.06
Ra-a65-66	4	8	—	2	20	70	10	3.50
Ra-c1-66	4	10	5	—	21	64	15	3.05
Ra-c4-66	4	9	—	3	24	64	12	2.66
Ra-a73-66	5	7	—	4	2	67	11	3.05
Ra-a14-66	5	11	—	—	20	69	11	3.45
Ra-a69-66	5	5	4	—	21	70	9	3.33
Ra-a33-66	5	6	4	—	20	70	10	3.50
Ra-b53-66	6	7	5	—	20	68	12	3.40
Ra-b48-66	6	7	—	—	22	70	7	3.18
Ra-a57-66	6	9	4	—	29	58	13	2.00
Ra-a96-66	6	8	—	—	24	68	8	2.83
Ra-a93-66	6	8	3	4	19	66	15	3.47
Ra-B4-66	7	6	—	—	43	51	6	1.19
Ra-B41-66	7	5	—	—	32	63	5	1.97
O-K-53	7′	4	4	—	17	75	8	4.41
O-K-15	7′	3	6	—	28	63	9	2.25
O-L-10	7′	6	5	—	25	64	11	2.50
O-J-65	7′	5	—	5	24	66	10	2.75
O-K-8′	8*	8	5	—	33	53	13	1.60
O-K-8	8*	11	3	—	33	53	14	1.61
O-K-9	8*	7	—	—	15	78	7	5.20
O-C-30	8	6	2	—	22	70	8	3.18
O-C-26	8	8	—	—	25	66	8	2.64
O-C-14	8	6	2	—	23	68	8	2.96
O-C-18	8	7	11	—	17	63	18	3.70
O-K-10	8	7	2	—	28	63	9	2.25
9-8/7/63	8′	12	2	—	23	62	14	2.70
16-8/23/60	8′	14	2	—	24	60	16	2.50
4-7/26/59	8′	7	7	—	24	62	14	2.58
16-7/18/60	9	11	—	—	25	64	11	2.56
15-8/18/59	9	5	—	8	25	61	8	2.44
14-7/2/60	9	7	5	—	21	67	12	3.19
5-9/20/61	9	13	—	2	25	68	15	2.72
O-b-41	—	11	2	2	27	57	14	2.11
O-I-1	—	8	5	7	64	16	20	4.00
O-G-92	—	7	5	7	65	17	19	3.82
O-H-49′	—	9	6	8	58	18	23	3.22
O-H-56	—	10	10	7	56	17	27	3.29
O-H-72	—	12	4	7	56	21	23	2.67
O-B-16	—	6	12	28	9	45	46	5.00

* Sulfide-rich samples not included in averages in Tables 2 and 4.

were used as standards for some minor elements. Correction techniques from Albee and Ray (1970) were used for all analyses. Replicate analyses on identical samples were performed to check the reproducibility of results between labs; no differences outside the standard errors were observed. Table 2 gives the average analysis for each grade.

Mössbauer spectral measurements were performed in the Mineral Spectroscopy Laboratories at the Massachusetts Institute of Technology and the University of Oregon. Sample preparation, experimental conditions, and fitting procedures are described in Dyar and Burns (1986). Results of the Mössbauer study, including peak parameters and interpretation, are presented in Dyar (1990). Table 3 presents the site occupancy data determined for the Maine samples.

Reliability of the Mössbauer data on biotite has been tested by Dyar (1984) and Dyar and Burns (1986). These reliability studies examined the effects of apparatus and fitting procedures by obtaining Mössbauer spectra of U.S. Geological Survey standards originally studied by Bancroft and Brown (1975). In addition, comparison of wet chemistry and Mössbauer results on several samples of synthetic annite and siderophyllite synthesized by Rebbert (1986) has recently been completed by Carolyn Rebbert (University of Oregon, personal communication) using the techniques and fitting procedures of Dyar and Burns (1986). Her work shows that the two analytical

TABLE 4. Summary of regional biotite data from Areas A and B

Item	Grade Zone no. on Table 1	LoGrt 1	MdGrt 2	UpGrt 3	LoSt 4	UpSt 5	Trans. 6	LoSil 7	LoSil 7′	UpSil 8	UpSil 8′	Kfs + Sil 9
Si	Oq-Ra	5.833	5.384	5.367	5.346	5.372	5.389	5.333	5.353	5.334	—	—
	Bryant Pond (JTC)	—	—	—	—	—	—	5.390	5.363	5.355	5.339	5.261*
	Bryant Pond (na)	—	—	—	—	—	—	—	—	—	5.512	5.328
ΣAl	Oq-Ra	3.493	3.525	3.561	3.519	3.534	3.516	3.557	3.530	3.498	—	—
	Bryant Pond (JTC)	—	—	—	—	—	—	3.468	3.539	3.490	3.460	3.446*
	Bryant Pond (na)	—	—	—	—	—	—	—	—	—	3.373	3.469
$^{[6]}$Al	Oq-Ra	1.103	1.136	1.145	1.071	1.100	1.099	1.089	1.099	1.044	—	—
	Bryant Pond (JTC)	—	—	—	—	—	—	1.051	1.103	1.048	1.008	0.917*
	Bryant Pond (na)	—	—	—	—	—	—	—	—	—	1.081	0.997
Mg/Mg + Fe_{tot}	Oq-Ra	0.384	0.377	0.410	0.450	0.474	0.468	0.460	0.404	0.410	—	—
	Bryant Pond (JTC)	—	—	—	—	—	—	0.478	0.450	0.440	0.433	0.430*
	Bryant Pond (na)	—	—	—	—	—	—	—	—	—	0.439	0.422
Mg/Mg + Fe^{2+}	Oq-Ra	0.415	0.408	0.442	0.482	0.506	0.500	0.492	0.435	0.442	—	—
	Bryant Pond (JTC)	—	—	—	—	—	—	0.510	0.481	0.472	0.464	0.461*
	Bryant Pond (na)	—	—	—	—	—	—	—	—	—	0.471	0.453
Ti	Oq-Ra	0.194	0.189	0.178	0.172	0.170	0.187	0.195	0.214	0.262	—	—
	Bryant Pond (JTC)	—	—	—	—	—	—	0.198	0.199	0.241	0.241	0.311*
	Bryant Pond (na)	—	—	—	—	—	—	—	—	—	0.246	0.367
Mn	Oq-Ra	0.022	0.015	0.009	0.009	0.009	0.009	0.009	0.013	0.019	—	—
	Bryant Pond (JTC)	—	—	—	—	—	—	0.009	0.012	0.017	0.017	0.023*
	Bryant Pond (na)	—	—	—	—	—	—	—	—	—	0.017	0.028
ΣFe^{2+} + Mg + Mn	Oq-Ra	4.299	4.242	4.269	4.392	4.320	4.282	4.311	4.221	4.196	—	—
	Bryant Pond (JTC)	—	—	—	—	—	—	4.346	4.290	4.253	4.318	4.317*
	Bryant Pond (na)	—	—	—	—	—	—	—	—	—	4.093	4.041
ΣVI	Oq-Ra	5.716	5.683	5.703	5.741	5.698	5.672	5.702	5.651	5.620	—	—
	Bryant Pond (JTC)	—	—	—	—	—	—	5.703	5.704	5.659	5.687	5.650*
	Bryant Pond (na)	—	—	—	—	—	—	—	—	—	5.518	5.509
Na/Na + K	Oq-Ra	0.024	0.045	0.033	0.052	0.051	0.051	0.046	0.044	0.038	—	—
	Bryant Pond (JTC)	—	—	—	—	—	—	0.046	0.045	0.043	0.043	0.037*
	Bryant Pond (na)	—	—	—	—	—	—	—	—	—	0.049	0.024
ΣXII	Oq-Ra	1.579	1.616	1.616	1.651	1.692	1.697	1.683	1.713	1.753	—	—
	Bryant Pond (JTC)	—	—	—	—	—	—	1.663	1.630	1.696	1.694	1.799*
	Bryant Pond (na)	—	—	—	—	—	—	—	—	—	1.783	1.823

Note: Data are based on 22 O, 8% $^{[4]}Fe^{3+}$, and 4% $^{[6]}Fe^{3+}$. Abbreviations: (na) = new analyses, (JTC) = from Cheney (1975), Oq-Ra = from Guidotti et al., (1988). All data adjusted to reflect new information on the average Fe^{3+} contents of these biotite samples over all grades considered.
* Only one specimen.

methods yield results that agree well within the known errors for the two methods.

Total Fe^{3+} varies little among the biotite that coexists with graphite and ilmenite from Areas A and B. With few exceptions, all samples contain roughly 12% of Fe_{tot} as Fe^{3+}. Figure 3 shows there is no systematic variation of $Fe^{3+}/\Sigma Fe$ over the metamorphic range studied.

In contrast, biotite from Area C, which coexists with magnetite, has distinctly higher Fe^{3+} contents. Five samples (O-I-1, O-G-92, O-H-49′, O-H-56, and O-H-72) contain roughly 22% ± 4 Fe^{3+} of the Fe_{tot}, which is attributed to the more oxidizing assemblage. This Fe^{3+} content is typical of biotite from other localities where biotite and magnetite coexist, such as northern New Mexico (Williams, 1987) and southern Arizona (Anthony and Titley, 1988). Most unusual is the Mössbauer data for sample O-B-16 (also from Area C), which contains 46% ± 3 Fe^{3+} of Fe_{tot}. The thin section from that sample showed that hematite is probably present, implying a more highly oxidized environment for this sample.

The Mössbauer results (Table 3) indicate that a majority of the Fe^{3+} in the biotite that coexists with graphite is located in the tetrahedral sites, despite the fact that all of these samples are Al saturated. Moreover, the great majority of samples studied from all three areas, A–C, contain tetrahedral Fe^{3+} in roughly the same amount, about 8 ± 3% of Fe_{tot}. Even in the magnetite-bearing samples that have considerably higher total Fe^{3+} contents, tetrahedral Fe^{3+} occurs in the 8 ± 3% range.

There is little variation in the distribution of Fe^{2+} between the M1 and M2 sites except in some of the samples from Zone 8 of Area A (e.g., O-K-8; Table 3). There is no apparent systematic variation of Fe^{2+} site occupancy with temperature, although peak positions are extremely consistent over the compositional range investigated. Few of the samples studied have the 2:1 Fe^{2+} site occupancy ratio in M2 vs. M1 expected in a totally disordered biotite. The majority of our samples have ratios of approximately 3:1. We were not able to resolve consistently the Fe^{3+} occupancy in both octahedral sites; however, the data do imply that Fe^{3+} is found in somewhat higher amounts in the M1 site.

Controls on Fe^{3+} and Fe^{2+} content and site assignments in biotite from metapelites

The literature on the Fe^{3+} content of biotite shows unequivocal proof that Fe^{3+} is widespread in biotite. Wet chemical analyses of trioctahedral micas considered in

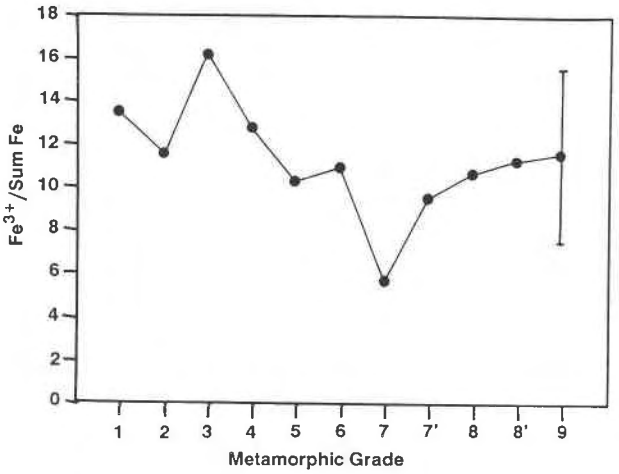

Fig. 3. $Fe^{3+}/\Sigma Fe$ ratio of biotite samples from limiting assemblages of Areas A and B, based on Oquossoc-Rangeley samples in this study and in Dyar (in press). Error bars on all points are ±3% as shown.

Foster's review (1960) show that of the 67 biotite samples for which Fe_2O_3 was determined, 66 contain Fe^{3+}. Foster (1960), Dodge et al. (1969), Guidotti (1984), Williams (1987), and virtually all others routinely assigned the Fe^{3+} to octahedral positions. This assumption may have been thermodynamically reasonable but ignores possible crystallochemical factors affecting $^{[4]}Fe^{3+}$. The literature on Mössbauer spectroscopic data on biotite also indicates the common presence of Fe^{3+}. For example, of 150 published spectra, 138 indicate the presence of Fe^{3+}. Therefore, one must conclude that biotite usually contains significant Fe^{3+}.

Most classical petrologic studies in which Fe^{3+} in biotite was considered (i.e., pre-1965 when only wet chemical analyses were available) gave a simplistic view of Fe^{3+}. Excluding a few studies (e.g., Chinner, 1960; Hounslow and Moore, 1967), the effects of metamorphic grade, the mineral assemblage, or the oxidation state were ignored. Then, development of the electron microprobe made it routine for petrologists to ignore completely Fe^{3+} in biotite or to assume that biotite from rocks such as the samples of Areas A and B bearing graphite and ilmenite contain virtually no Fe^{3+}. This situation continues, although Guidotti (1984) showed that published wet chemical analyses indicate that biotite coexisting with graphite typically contains about 10% of its Fe as Fe^{3+} and that biotite from magnetite-bearing rocks has about 20% of its Fe as Fe^{3+}.

This study suggests that the amount and location of Fe^{3+} in biotite (and possibly in other common rock-forming phases) is controlled by both petrologic and crystallochemical factors.

Petrologic controls. The Mössbauer data for the biotite samples of Areas A, B, and C show that all have about 8 ± 3% of their Fe_{tot} as $^{[4]}Fe^{3+}$. This amount holds quite steady regardless of all petrologic factors. Below, we suggest that this relatively constant amount of $^{[4]}Fe^{3+}$ is required by crystallochemical factors.

The Mössbauer data indicate that biotite from the reduced environments of Areas A and B usually has only small, relatively uniform amounts of $^{[6]}Fe^{3+}$ present (about 4% of Fe_{tot}). This is so regardless of metamorphic grade or variations among the limiting assemblages considered (see Appendix A for a statistical analysis of errors for the variation of $^{[4]}Fe^{3+}$ and $^{[6]}Fe^{3+}$ as a function of metamorphic grade for the biotite of Areas A and B).

Biotite from Area C coexists with magnetite (also with hematite in one sample), which implies a more oxidizing environment. Apparently in response to this increase in oxidation state, these biotite samples not only contain the usual $^{[4]}Fe^{3+}$, but also contain greater amounts of $^{[6]}Fe^{3+}$ (an additional 14% of Fe_{tot}). The biotite (O-B-16) coexisting with hematite contains an even greater amount of Fe^{3+} (46% of Fe_{tot}), thereby reflecting even higher f_{O_2} conditions for that specimen. Thus the oxidation state during crystallization that can be inferred on the basis of the coexisting opaque minerals is the only petrologic factor that influences the amount of $^{[6]}Fe^{3+}$ in biotite. The independence of $^{[6]}Fe^{3+}$ content from metamorphic grade also includes independence of factors controlled by metamorphic grade: silicate mineral assemblage, $Mg/(Mg + Fe^{2+} + Fe^{3+})$ ratio, and TiO_2 content.

In contrast to the case for $^{[6]}Fe^{3+}$, the amount of $^{[4]}Fe^{3+}$ appears to be independent of any petrologic factor whatsoever. It averages about 0.196 cations per formula unit (ca. 8 ± 3% of Fe_{tot}) for all biotite samples in Areas A, B, and C as well as for sample O-b-41, a granite. If Fe^{3+} in biotite were a function only of oxidation state, Fe^{3+} content would range from nil to about 50% (above which the structure would not be stable). Instead, the data suggest a plateau with a Fe^{3+} content averaging near 12 ± 3% of Fe_{tot} (specimens from Areas A and B), another plateau of values ranging between 19 and 27% (the magnetite-bearing rocks of Area C) and a single specimen with a Fe^{3+} content near 50% (the hematite-bearing specimen of Area C). Of particular interest is the absence of biotite with less than about 12% of Fe_{tot} as Fe^{3+} and the location of much of this Fe^{3+} in tetrahedral sites despite the rocks being Al saturated. The observations suggest structural controls of some type on $^{[4]}Fe^{3+}$.

Crystallochemical controls on Fe^{3+} and Fe^{2+} site location. The Mössbauer results presented above can be accepted directly for site assignments of Fe^{3+} and Fe^{2+} in biotite. However, it is important to consider site assignment also in terms of biotite crystal chemistry, as doing so will enable us to gain insight into important thermodynamic and petrologic constraints related to the solution properties of biotite.

Crystallochemical arguments on the need for Fe^{3+} to meet structural requirements for some biotite compositions already exist. For example, Hazen and Wones (1972) invoked structural misfit to justify the need for about 12% octahedral Fe^{3+} in synthetic annite. With its high Fe^{2+} content, annite has large octahedral sheets owing to

the large ionic radius of Fe^{2+}. The smaller Fe^{3+} in octahedral positions is required to shrink the octahedral sheet sufficiently to articulate with the tetrahedral sheet.

For common, natural biotite, the presence of Al, Ti, and Mg as well as Fe^{2+} in the octahedral sites, plus the relative ease of tetrahedral rotation would seem to obviate gross scale structural arguments for either tetrahedral or octahedral assignment of Fe^{3+}.

However, the observed $^{[4]}Fe^{3+}$ may be understandable if local scale distortions related to octahedral vacancies are considered. It is widely known that most naturally occurring biotite contains vacancies in the octahedral sheets. Such vacancies are commonly (and incorrectly) blamed on the failure to analyze for Fe^{3+}. In fact, recalculations of electron microprobe analyses that take Mössbauer-determined ratios of Fe^{3+}/Fe_{tot} into account give slightly increased numbers of vacancies owing to adjustment for Fe_2O_3. The frequency of such vacancies is not great enough to cause large scale structural distortions (0.1–0.4 vacancies per six octahedral sites are common).

Vacant octahedra with hypothetical ionic radii of 0.80 Å (Guggenheim, 1984) may cause significant distortions in the local scale structure, particularly if adjacent to much smaller octahedra occupied by 3^+ or 4^+ cations. As noted by Bailey (1984, p. 19), the detailed shapes of the tetrahedra in micas are influenced by the size and charge of the adjacent octahedral cations or vacancies. An ideal SiO_4 tetrahedron has all three O_{apical}-Si-O_{basal} angles (angle τ) at 109°28′, but Lee and Guggenheim (1981) have shown that in dioctahedral micas, one of these angles is about two degrees greater than the other two. The larger angle is related to the octahedral vacancy in a systematic fashion.

In the case of biotite (average $\tau \sim 110.3°$; Bailey, 1984, Table 1), one might expect deviations of this angle among tetrahedra associated with the randomly occurring octahedral vacancies of biotite (random at least in annite, Hazen and Burnham, 1973), especially if adjacent octahedra contain small, high valence cations such as Al^{3+} or Ti^{4+}. Indeed, considering the complexity of the octahedral sheet in biotite (random vacancies, presence of small, high valence cations, concentration of Fe^{2+} in the M2 octahedron, etc.), one might expect that different tetrahedra would show differing degrees of distortion. Such a model involves accomplishing articulation of the tetrahedral and octahedral sheets on a very local scale. Gross scale articulation would be accomplished by other adjustments such as tetrahedral rotation (See Bailey, 1984, p. 16 ff. for a full discussion).

For our purposes, it seems reasonable to suggest that Fe^{3+} might displace Al^{3+} from the occasional, more distorted tetrahedra adjacent to some of the octahedral vacancies. In our samples it appears that the number of $^{[4]}Fe^{3+}$ roughly equals the number of octahedral vacancies. Thus, tetrahedral distortions caused by adjacent octahedral vacancies may be a structural feature leading to the common observation of at least 8% Fe^{3+} in the tetrahedral sites of our biotite.

Indeed, that all 52 biotite samples in this study contain $^{[4]}Fe^{3+}$ in roughly equivalent amounts of 8% of Fe_{tot}, regardless of f_{O_2} and total Fe^{3+} in the biotite, implies a crystallochemical rather than petrologic control. Because all samples contain roughly the same numbers of octahedral vacancies, the 8% value may represent a baseline Fe^{3+} content for typical, naturally occurring biotite. In contrast, the amount of $^{[6]}Fe^{3+}$ is probably largely independent of structural constraints and is mainly a reflection of f_{O_2}. The only clearly crystallochemical aspect of $^{[6]}Fe^{3+}$ would be that related to the need for charge balance.

As noted in Table 3, Fe^{2+} is strongly partioned into M2, except for samples O-K-8, O-K-8′, and O-K-9, all of which are very Mg rich. Unfortunately, the pattern for these three samples is not systematic and thus provides no insights to determine if Fe^{2+} or Mg is exhibiting a site preference.

Crystallochemical and petrologic implications

Crystallochemical implications. In this section we use the data and ideas discussed above, along with other published results, to establish better constrained site substitution models (SSMs) for the biotite groups. Because of the existing petrologic constraints (mainly, bulk composition), the total Fe is quite similar in all samples considered (excluding O-K-8, O-K-8′, and O-K-9). Hence, the amounts of Fe^{3+} can also be presented in terms of cations per site and/or per formula unit.

Specifically, all of our samples uniformly have 0.196 Fe^{3+} cations per formula unit in the tetrahedral sites (roughly comparable to the number of octahedral site vacancies). The biotite of Areas A and B (graphitic rocks) contains a uniformly small amount of $^{[6]}Fe^{3+}$ (average of 0.11 cations per formula unit) whereas the biotites of Area C (magnetite present) uniformly have about 0.318 Fe^{3+} in the octahedral sites. The one biotite from Area C coexisting with hematite has 0.686 Fe^{3+} atoms per formula unit. Because one can define base levels for the amount of $^{[4]}Fe^{3+}$ and $^{[6]}Fe^{3+}$ within a given group of samples, constant amounts of $^{[4]}Fe^{3+}$ or $^{[6]}Fe^{3+}$ can be assumed when formulating activity models, etc. This holds in detail only for the biotite samples from Areas A and B. The data for biotite from Area C are too few for similar treatment.

Finally, some early studies on micas (Brown and Norrish, 1952; White and Burns, 1963) suggested the existence in micas of the substitution

$$(K^+, Na^+) \rightleftharpoons H_3O^+. \quad (1)$$

Recently, new analytical and statistical studies indicating excess H_2O in micas have provided important additional support for this substitution [Dyar, 1988 (fast neutron analysis); Hervig and Peacock, 1989 (ion microprobe); Loucks, in preparation (statistical analysis of wet chemical data)].

Thus, interlayer site vacancies shown in Guidotti et al. (1988) could be a reflection of Substitution 1. This sub-

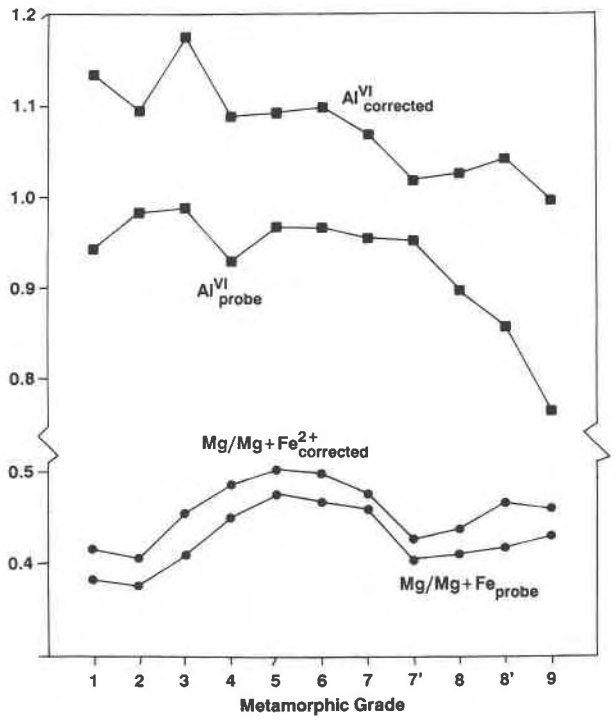

Fig. 4. Illustration of the manner in which biotite Mg/(Mg + Fe) ratio and $^{[6]}Al$ content are shifted owing to inclusion of Fe^{3+} data, based on data from Dyar, 1990. Error bars on both quantities are roughly ±0.01 formula units.

stitution does not require the interlayer site charges to be involved with balancing octahedral site charges either on a gross scale or in terms of local charge balance. This aspect may be of significance considering the relatively dispersed nature of the charges on the cations in the interlayer sites and their distance from the octahedral cations. If the observed systematic variation of the total number of interlayer cations (see Table 4) represented a systematic variation in the total number of interlayer vacancies, one might expect a concomitant variation of $^{[4]}Al$ relative to Si. No such variation occurs for the biotite of western Maine. Wang and Banno (1987) have also discussed deficiencies in the interlayer cations, and they did argue for a relationship involving concomitant substitutions in other sites.

We suggest that the increase of the $\Sigma(K + Na + Ba)$ in biotite over the range of grades found in Areas A and B (see Table 4) reflects a temperature control on Substitution 1 (see also Hervig and Peacock, 1989). That increase of temperature appears to drive Substitution 1 toward dehydration could be taken as support for its existence. If Substitution 1 does occur in biotite (and also presumably muscovite), it suggests progressive dehydration of micas well before their upper stability limits are reached.

Site substitution models for biotite from Areas A and B. Integration of the above discussion with the site substitution models (SSMs) proposed in Guidotti et al. (1988) for biotite from western Maine enables us to remove more of the ambiguity from their models. Table 4 reviews key data for biotite from Area A (Guidotti et al., 1988); biotite from Area B (Cheney, 1975), and new data extending Area B well into the potassium feldspar + sillimanite zone. The data of Cheney (1975) overlaps in grade with that of Guidotti et al. (1988) and the new data. All data are from Al-, Si-, and Ti-saturated limiting assemblages.

Guidotti et al. (1988) detected a number of grade-controlled compositional variations in biotite (lower garnet zone to upper sillimanite zone). Table 4 summarizes these variations and shows how the patterns continue for the biotite from the higher grades in Area B. Some systematic differences exist in the absolute values for the overlapping grades, e.g., note the $Mg/(Mg + Fe_{tot})$ ratios. These may be due to actual differences in metamorphic conditions (P, T, or aH_2O) or to analytical procedure. Regardless of the cause, the projected patterns for the grade to grade variation compare very well for both areas and can be integrated for purposes of developing a SSM for the biotite samples from Areas A and B combined.

The values in Table 4 have been adjusted for 4% octahedral and 8% tetrahedral occupancy of Fe^{3+}, the averages for all Area A and Area B samples studied. Hence, some of the patterns described in Guidotti et al. (1988) are shifted systematically. For example, the $Mg/(Mg + Fe^{2+})$ ratio is increased owing to subtraction of ~12% of the Fe that is Fe^{3+}, also $^{[6]}Al$ increases owing to the displacement by $^{[4]}Fe^{3+}$ of the Al previously allotted to tetrahedral sites (Fig. 4).

Guidotti et al. (1988) recognized several substitutions clearly related to metamorphic reactions produced by the increase of grade. These include (a) $Mg^{2+} \leftrightharpoons Fe^{2+}$, (b) $Na^+ \leftrightharpoons K^+$, and (c) $Mn^{2+} \leftrightharpoons (Mg^{2+}, Fe^{2+})$.

They also noted systematic compositional variations of Area A biotite as grade increased. These include (A) interlayer site-occupancy increases, (B) the total octahedral cations and $\Sigma(Fe + Mg + Mn)$ decrease, and (C) Ti increases at grades above the staurolite zone and increases rapidly at the highest grades. It is apparent that (a)–(c) and (A)–(C) continue through the higher grades of Area B.

Many workers have recognized (a)–(c) and (A)–(C) and suggested SSMs to explain the patterns (see references in Guidotti, 1984). However, unambiguous SSMs were not possible because of incomplete data on Fe^{3+} and its site assignment and also lack of information on the O content which, as developed in Dyar (1988), bears on the H_3O^+ substitution in the interlayer site. Hewitt and Abrecht (1986) emphasized the inherent ambiguity of the SSMs proposed without adequate constraints to restrict the number of substitution equations.

The substitutions or variations proposed by Guidotti et al. (1988) [(a)–(c) and (A)–(C), above] appear fully compatible with all of the new data. Two additional substitutions will explain essentially all of the compositional variation not covered by the substitutions or variations proposed by Guidotti et al. (1988). As discussed above,

one is Substitution 1. It appears to be superimposed on the Na-K substitution which is controlled by grade.

The other substitution, which is better supported by the now more constrained data, is:

$$\text{Ti} + \text{octahedral vacancy} \leftrightharpoons 2(R^{2+}) \quad \text{(where } R^{2+} \text{ is } Fe^{2+}, \text{ Mg, or Mn).} \qquad (2)$$

Guidotti (1984) noted that many workers have suggested Substitution 2 to explain compositional variations of biotite in metamorphic rocks like those in Areas A and B at metamorphic grades exceeding the lower staurolite zone. However, even when Al, Si, and Ti were held at their saturation levels, ambiguities persisted because of lack of information on interlayer site-occupancy and Fe^{3+}. In this study we have suggested that the interlayer substitutions are not related to the octahedral site substitutions, and that $^{[4]}Fe^{3+}$ and $^{[6]}Fe^{3+}$ remain essentially constant over the range of grades considered. Moreover, Table 4 shows that as grade increases, the increase in Ti and the number of vacancies is nearly balanced vs. the decrease in $\Sigma(Fe^{2+} + Mg + Mn)$, both in terms of numbers of cations and positive charges. For local charge balance reasons one might expect a Ti^{4+} and vacancy to be adjacent to each other.

Addition of Substitutions 1 and 2 to those proposed by Guidotti et al. (1988) seems to prove an unambiguous SSM for the biotite of the limiting assemblages in Areas A and B, at least at staurolite and higher grades. For the nonlimiting assemblages, ambiguity still persists. In the limiting assemblages, minor substitutions involving ΣAl and $^{[4]}$Al are possible, but the data are too limited to establish them unequivocally. For the most part, Si, $^{[4]}$Al, ΣAl, $^{[6]}$Al, $^{[4]}Fe^{3+}$, and $^{[6]}Fe^{3+}$ are essentially constant over the range of metamorphic grades of Areas A and B owing to Al and Si saturation and constant oxidation levels.

The marked increase of Ti at grades above the upper staurolite zone results from Substitution 2, apparently reflecting a temperature-controlled expansion of the Ti saturation limit in biotite. This is also reflected by an independent petrographic observation of Evans and Guidotti (1966); the modal amount of ilmenite decreases as grade increases from the upper sillimanite zone to potassium feldspar + sillimanite zone (zones 8′ to 9 herein). Such a modal decrease of ilmenite is easily understood as outlined in Figure 5. It is important to note that Substitution 2 applies rigorously only to biotite coexisting with muscovite. Guidotti (1984, p. 436) noted that in biotite from grades above the stability of muscovite, a substitution involving replacement of $^{[6]}$Al by Ti becomes important also. Care should be taken to avoid confusing Substitution 2 with the Ti substitution

$$^{[6]}(R^{2+}) + 2\text{Si} \leftrightharpoons {}^{[6]}(\text{Ti}) + {}^{[4]}(2\text{Al}). \qquad (3)$$

Guidotti et al. (1977b) provided evidence for Substitution 3 proceeding to the left when sulfide-silicate reactions cause extreme Mg enrichment of biotite. Careful selection of samples for this study has excluded this substitution, thereby enabling us to attribute the observed variation of Ti almost wholly to Substitution 2.

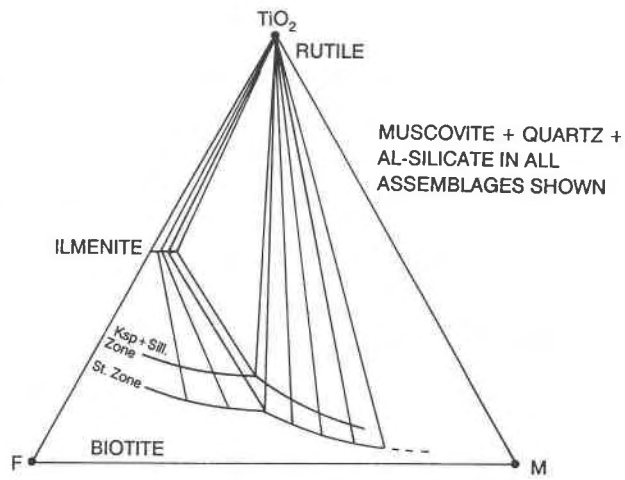

Fig. 5. Schematic illustration of the manner in which the Ti saturation surface in biotite coexisting with ilmenite shifts as metamorphic grade increases.

Abrecht and Hewitt (1988) have recently shown experimentally that Substitutions 2 and 3 are the most important ways by which Ti enters biotite. Data from natural parageneses, however, suggest a difference in terms of the relative importance of those two substitutions when $Mg/(Mg + Fe^{2+})$ ratios are considered. Such data clearly show that Substitution 3 is driven to the left at high values of $Mg/(Mg + Fe^{2+})$ ratio. At intermediate ratios, Substitution 2 is the primary substitution by which the solubility of Ti in biotite increases at grades increasing above the upper staurolite zone.

Although unambiguous SSMs are possible for the biotite of Areas A and B limiting assemblages formed at upper staurolite zone and higher, they remain ambiguous for biotite formed at lower garnet zone to staurolite zone. The substitutions suggested in Guidotti et al. (1988) certainly remain valid and Substitution 1 is also quite likely. However, the substitutions by which Ti enters biotite in these lower grades of metamorphism are ambiguous. Similarly, the substitutions responsible for the octahedral vacancies present and the excess of trivalent octahedral cations over that owing to a simple Tschermak exchange (see Guidotti, 1984, p. 437 for a discussion) remain unresolved. Various combinations of substitutions can be formulated, but no set can be designated as the most likely. This problem arises because, in contrast to the situation at staurolite grade and higher, there is virtually no systematic variation of Ti, Σ octahedral cations, etc., over the lower grade range. Hence, no opportunity exists to ascertain what cations vary in response to other cations or site occupancies.

Petrologic implications

The data and crystallochemical features discussed above have important petrologic implications for mineral equi-

libria involving biotite in pelitic schists. Included would be the thermodynamic formulations involving biotite that are aimed at geothermometry, geobarometry, or calculation of fluid compositions during metamorphism. These implications can be distinguished at two levels.

Level one is the numerical adjustment required in the $Mg/(Mg + F_{tot})$ ratios when accounting for the proportion of total Fe that is actually Fe^{3+}. Clearly this adjustment will change the $Mg/(Mg + Fe^{2+})$ ratio (see Fig. 4). Dyar et al. (1987) showed that for graphite-bearing rocks, adjustment of the $Mg/(Mg + Fe^{2+})$ ratio of biotite used in garnet-biotite geothermometry could lower calculated temperatures by up to 45° C. However, caution is required because the original experimental calibrations of the garnet-biotite geothermometer (Ferry and Spear, 1978) may have involved biotite with Fe^{3+} contents typical of graphite-bearing assemblages. This question remains unresolved. For biotite coexisting with magnetite or hematite, e.g., Area C rocks, the adjustment of $Mg/(Mg + Fe_{tot})$ to $Mg/(Mg + Fe^{2+})$ causes large changes in the temperatures calculated from garnet-biotite geothermometry. Clearly, any similar thermodynamic calculations involving Fe-bearing biotite must take into account the oxidation state of the rocks, at least at the level that can be inferred from the suite of coexisting opaque minerals.

The other level of petrologic implications is less straightforward. It involves crystallochemical aspects bearing on: (1) formulation of ideal activity models, (2) deviation of biotite solid solutions from ideality, and (3) consideration of the existence of annite as an end-member of the biotite solid solution.

Ideal activity models. Thermodynamic formulations involving equilibria among rock-forming minerals build upon the relationship $u_i = u_i^0 + RT \ln a_i$, in which a_i is the activity of a component in a solution phase participating in the equilibria. The a_i may be restated as X_i or $X_i\gamma_i$ depending upon whether the solution behaves in an ideal or nonideal fashion. X_i is termed the ideal mixing activity or the thermodynamic mole fraction (Powell, 1977).

In formulating X_i, it is assumed that constituents mix randomly within each site. For a phlogopite end-member component, the X_{phl} in some biotite might be written as $(X_K)\cdot(X_{Mg})^3\cdot(X_{(OH)})^2$ for the mixing that takes place on the interlayer, octahedral and (OH) sites, respectively. As discussed in Nordstrom and Munoz (1985) and Powell (1977, 1978) a normalization term commonly is applied to cases like phlogopite in order to account for the nature of the Al-Si ordering assumed for the tetrahedral sites. Moreover, in contrast with other discussions, Powell (1978) suggests an X_{Ph} formulation which includes a distinction between mixing on the M1 and M2 octahedral sites.

Results from this study suggest that common pelitic biotite has the following crystallographic site positions and cations occupancies: $^{[12]}(K,Na,Ba,H_3O,\square)$, $^{[6]}(Mg,Fe^{2+},Fe^{3+},Al,Mn,Ti,\square)_3$ $^{[4]}(Al_xFe^{3+}_ySi_{4-(x+y)}O_{10})$ $(OH,F)_2$. Our data suggests that Fe^{2+} is not randomly distributed over the M2 and M1 sites thereby supporting Powell's X_i model for the components of biotite. Moreover, the presence of significant tetrahedral Fe^{3+} even in biotite from Al-saturated rocks indicates that normalization to an Al/Si ratio of 1:3 in the tetrahedral sites is unrealistic.

Evidence of deviation from ideality by biotite solid solutions. Because of the chemical complexity of phases such as biotite and the paucity of data, we emphasize that our remarks apply only to biotite from pelitic assemblages which are saturated with Al, Si, and Ti and at oxidation levels characteristic of rocks containing graphite or magnetite. Our discussion will be in terms of specific sites and then between sites.

1. Tetrahedral sites: although our data provide no indications of deviations from ideality for the substitutions of Al for Si in the tetrahedral sites, our model to explain the occurrence of $^{[4]}Fe^{3+}$ does suggest local scale ordering keyed to the location of octahedral vacancies. This implies a clear deviation from the conditions implicit in formulating the tetrahedral X_a term for an ideal activity (Powell, 1978).

2. Octahedral sites: in general, petrologists consider mixing on the octahedral sites of biotite to be nearly ideal. Our data, combined with that presented in Guidotti et al. (1975, 1977b, 1988) suggests several possible deviations from such ideal mixing. The 3:1 concentration of Fe^{2+} in M2 vs. M1 octahedra implies a deviation from ideal mixing over all three sites, but as noted earlier one cannot determine exactly which cations are ordered. Alternatively, if one considers the M2 and M1 octahedra as intrinsically different, (as done by Powell, 1978) then one must assess whether mixing is ideal within each site respectively. Our data do not bear on this latter possibility.

Data on multisite substitutions in biotite from Areas A and B provide evidence for nonideality by at least one common substitution in biotite. First, observations of Guidotti et al. (1977b) suggested that in Al-, Ti-, and Si-saturated biotite samples, a combination of size adjustment and charge-balance requirements occur in Mg-rich biotite that inhibits Ti from substituting into octahedral sites. In essence, Substitution 3 is forced to the low Ti side. This implies that Substitution 3 is not ideal but depends upon the Mg/Fe ratio of the biotite; i.e., the degree of Ti substitution depends upon the relative amounts of other cations present in the octahedral site. Moreover, this antipathy between Ti and Mg at high $Mg/(Mg + Fe^{2+})$ ratios suggests that at high Ti contents there may be a tendency for Ti to replace Mg via Substitution 2. Alternatively, one might view Ti entering biotite via Substitution 2 to be selectively replacing Mg.

Annite as an end-member of biotite. The ideal annite end-member of biotite has the composition $KFe^{2+}_3(AlSi_3O_{10})(OH)_2$ and is named after a reported occurrence on Cape Ann, Massachusetts. However, Dyar and Burns (1986) have shown that this annite has 55% of its Fe as Fe^{3+}. Hazen and Wones (1972) have discussed the structural aspects of having all Fe^{2+} in the octahedral sites, and the review of Guidotti (1984) has emphasized that all metamorphic biotite samples have significant $^{[6]}Al$ and $^{[4]}Al$ in excess of one per formula unit.

In the context of this work, a key observation is that

even biotite coexisting with graphite contains significant Fe^{3+}, albeit mainly in the tetrahedral sites. Biotite from magnetite-bearing rocks contains significant $^{[6]}Fe^{3+}$ as well as $^{[4]}Fe^{3+}$. A generalization that emerges is that the use of annite as a thermodynamic end-member for equilibrium calculations may be significantly in error, certainly for pelitic schists. Holdaway (1982) has discussed the desirability of defining thermodynamic end-members that have more direct relevance to the equilibria in both natural and experimental systems.

Finally, data for biotite in pelitic schists suggest a need to rethink the details of redox and exchange reactions involving Fe^{3+}. Specifically, for pelitic schists, attributing the incorporation of Fe^{3+} in minerals like biotite solely to redox reactions may need some reconsideration. Its presence might be more simply interpreted via crystallochemical arguments (e.g., $^{[4]}Fe^{3+}$) and coexistence with Fe^{3+}-saturating phases (e.g., magnetite and the saturation amount of $^{[6]}Fe^{3+}$ in conjunction with other cation substitutions). Addressing these possibilities will require consideration of Fe^{3+} in the phases coexisting with biotite. The authors are actively investigating some of these other minerals (ilmenite, staurolite, muscovite, and chlorite at present). Data in the literature (reviewed in Guidotti, 1984) already suggest that muscovite has a higher Fe^{3+}/Fe^{2+} ratio than minerals like biotite or chlorite.

Conclusions

This study has provided several specific insights with respect to chemical, petrologic, and crystallochemical aspects of biotite from pelitic schists. However, the most important conclusions to be drawn from this study may be of more general nature. They include:

1. Solution phases in metamorphic rocks may be more complex in terms of cation site substitution and deviations from ideality than assumed by petrologists. Moreover, the nature of the complexity probably varies depending upon the composition range considered for the solid solution and metamorphic grades considered. These statements are made with reference to biotite but will probably also apply to other micas, chlorites, and amphiboles.

2. Because of these complexities, most thermodynamic formulations involving these phases are incomplete to varying extents. The extent of the resulting problems cannot be defined in most cases, but certainly great caution is warranted for formulations involving a series of several sequential assumptions regarding the nature of the solution properties of the phases involved. In at least the case of garnet-biotite geothermometry as applied to magnetite-bearing rocks, it is clear that if no account is given to Fe^{3+} in the biotite, the temperatures calculated must be specious.

3. Because of the difficulties noted above, we urge that more effort be directed at studying the solution properties of minerals, both experimentally and in natural parageneses. For example, recently Kohn and Spear (1989) have suggested that poorly constrained activity models may be a major source of pressure uncertainty resulting from calculations using cation exchange geobarometers. The approaches provided by crystallographers and mineral physicists will be of particular importance for such studies, especially if they are set within a petrologic context.

Acknowledgments

Reviews of this paper by E.S. Grew, M.H. Reed, M.J. Holdaway, and S. Guggenheim have been very helpful and are greatly appreciated, as is the skillful assistance of Lucy Biggs in preparation of this manuscript. The authors are, of course, responsible for any remaining inadequacies in this work.

The work of C.V.G. on biotite and other solid solution minerals has been supported by NSF Grants EAR-820050, EAR-8204254, and EAR-8817066. The work of M.D.D. for Mössbauer study of rock forming minerals has been supported by NSF Grants EAR-8709359 and EAR-8816935. The authors gratefully acknowledge this support. Acknowledgment is also made to the donors of The Petroleum Research Fund, administered by the A.C.S., for additional support of this research through grant 19217-G2 to M.D.D.

References cited

Abrecht, J., and Hewitt, D.A. (1988) Experimental evidence on the substitution of Ti in biotite. American Mineralogist, 73, 1275–1284.

Albee, A.L., and Ray, L. (1970) Correction factors for electron microanalysis of silicates, oxides, carbonates, phosphates, and sulphates. Analytical Chemistry, 42, 1408–1414.

Al-Mishwt, A. (1972) Contact metamorphism and polymetamorphism in northwestern Oquossoc quadrangle, Maine. M.S. thesis, University of Wisconsin, Madison, Wisconsin.

Anthony, E.Y., and Titley, S.R. (1988) Progressive mixing of isotopic reservoirs during magma genesis at the Sierrita porphyry copper deposit, Arizona: Inverse solutions. Geochimica et Cosmochimica Acta, 52, 2235–2249.

Bailey, S.W. (1984) Crystal chemistry of the true micas. Mineralogical Society of America Reviews in Mineralogy, 13, 13–60.

Bancroft, G.M., and Brown, J.R. (1975) A Mössbauer study of coexisting hornblendes and biotites: Quantitative Fe^{3+}/Fe^{2+} ratios. American Mineralogist, 60, 265–272.

Brown, G., and Norrish, K. (1952) Hydrous micas. Mineralogical Magazine, 29, 929–932.

Cheney, J.T. (1975) Mineralogy and petrology of lower sillimanite through sillimanite + K-feldspar zone, pelitic schists, Puzzle Mountain area, Northwest Maine, 291 p. Ph.D. thesis, University of Wisconsin, Madison, Wisconsin.

Cheney, J.T., and Guidotti, C.V. (1979) Muscovite-plagioclase equilibria in sillimanite + quartz-bearing metapelites, Puzzle Mountain area, northwestern Maine. American Journal of Science, 279, 411–434.

Chinner, G.A. (1960) Peltic gneisses with varying ferrous/ferric ratios from Glen Clova, Angus, Scotland. Journal of Petrology, 1, 178–217.

Dodge, F.C.W., Smith, V.C., and Mays, R.E. (1969) Biotites from granitic rocks of the central Sierra Nevada batholith, California. Journal of Petrology, 10, part 2, 250–271.

Dyar, M.D. (1984) Precision and interlaboratory reproducibility of measurements of the Mössbauer effect in minerals. American Mineralogist, 69, 1127–1144.

——— (1988) Direct evidence of hydronium substitution in biotite. Annual Meeting of the Geological Society of America Abstract with Programs, A102.

——— (1990) Mössbauer spectra of biotite from metapelites. American Mineralogist, 75, 656–666.

Dyar, M.D., and Burns, R.G. (1986) Mössbauer spectral study of ferruginous one-layer trioctahedral micas. American Mineralogist, 71, 955–965.

Dyar, M. Darby, Grover, T.W., Rice, J.M., and Guidotti, C.V. (1987) Presence of ferric iron and octahedral ferrous ordering in biotites from pelitic schists. Implications for garnet-biotite geothermometry. Annual

Meeting of the Geological Society of America Abstract with Program, November 1987.
Evans, B.W., and Guidotti, C.V. (1966) The sillimanite-potash feldspar isograd in western Maine, U.S.A. Contributions to Mineralogy and Petrology, 12, 25–62.
Faye, G.H. (1968) The optical absorption spectra of certain transition metal ions in muscovite, lepidolite and fuchite. Canadian Journal of Earth Science, 5, 31–38.
Ferry, J.M., and Spear, F.S. (1978) Experimental calibration of Fe and Mg partitioning between biotite and garnet. Contributions to Mineralogy and Petrology, 66, 113–117.
Foster, C.T. (1977) Mass transfer in sillimanite-bearing pelitic schists near Rangeley, Maine. American Mineralogist, 62, 727–746.
Foster, M.D. (1960) Interpretation of the composition of trioctahedral micas. U.S. Geological Survey Professional Paper 354-B.
Green, J.C. (1963) High-level metamorphism of pelitic rocks in northern New Hampshire. American Mineralogist, 48, 991–1023.
Green, J.C., and Guidotti, C.V. (1968) The geology of the Boundary Mountains Anticlinorium in northern New Hampshire and northwestern Maine. In E-an Zen, W.S. White, J.B. Hadley, and J.B. Thompson, Jr., Eds., Studies of appalachian geology, p. 255–266. Wiley, New York.
Guggenheim, S. (1984) The brittle micas. Mineralogical Society of America Reviews in Mineralogy, 13, 61–104.
Guidotti, C.V. (1963) Metamorphism of the pelitic schists in the Bryant Pond quadrangle, Maine. American Mineralogist, 48, 772–791.
——— (1970a) The mineralogy and petrology of the transition from lower to upper sillimanite zone in the Oquossoc area, Maine. Journal of Petrology, 11, 277–336.
——— (1970b) Metamorphic petrology, mineralogy, and polymetamorphism in a portion of N.W. Maine. In G.M. Boone, Ed., Guidebook for field trips in the Rangeley Lakes–Dead River Basin region, Western Maine. New England Intercollegiate Geology Conference, 62nd Annual Meeting, Field Trip B2, 1–23.
——— (1973) Compositional variation of muscovite as a function of metamorphic grade and assemblage in metapelites from N.W. Maine. Contributions to Mineralogy and Petrology, 42, 33–42.
——— (1974) Transition from staurolite to sillimanite zone, Rangeley quadrangle, Maine. Geological Society of America Bulletin 85, 475–490.
——— (1977) The geology of the Oquossoc 15′ quadrangle, west central Maine. Maine Geological Survey, Open file no. 77-2, 26 p., report and map. Augusta, Maine.
——— (1978) Compositional variation of muscovite in medium to high grade metapelites of northwestern Maine. American Mineralogist, 63, 878–884.
——— (1984) Micas in metamorphic rocks. In S.W. Bailey, Ed., Micas. Mineralogical Society of America Reviews in Mineralogy, 13, 357–467.
——— (1985) Metamorphic map of Maine. In P.H. Osberg, A.M. Hussey II, and G.M. Boone, Eds., Geologic map of Maine, Maine Geological Survey, Augusta, Maine.
Guidotti, C.V., Herd, H.H., and Tuttle, C.L. (1973) Composition and structural state of K-feldspars from K-feldspar + sillimanite grade rocks in northwestern Maine. American Mineralogist, 58, 705–716.
Guidotti, C.V., Cheney, J.T., and Conatore, P.D. (1975) Interrelationship between Mg/Fe ratio and octahedral Al content in biotite. American Mineralogist, 60, 849–853.
Guidotti, C.V., Cheney, J.T., and Henry, D.J. (1977a) Sulfide-silicate phase relations in metapelites of northwestern Maine. Eos, 58, 524.
Guidotti, C.V., Cheney, J.T., and Guggenheim, S. (1977b) Distribution of titanium between coexisting muscovite and biotite in pelitic schists from northwestern Maine. American Mineralogist, 62, 438–448.
Guidotti, C.V., Cheney, J.T., and Henry, D.J. (1988) Compositional variation of biotite as a function of metamorphic reactions and mineral assemblage in the pelitic schists of western Maine. American Journal of Science, 288-A, 270–292.
Hazen, R.M., and Burnham, C.W. (1973) The crystal structures of one-layer phlogopite and annite. American Mineralogist, 58, 889–900.
Hazen, R.M., and Wones, D.R. (1972) The effect of cation substitution on the physical properties of trioctahedral micas. American Mineralogist, 57, 103–125.
Henry, D.J. (1981) Sulfide-silicate relations of the staurolite grade pelitic schists, Rangeley quadrangle, Maine. Ph.D. thesis, University of Wisconsin, Madison, Wisconsin.
Hervig, R.L., and Peacock, S.M. (1989) Water and trace elements in coexisting muscovite and biotite from metamorphic rocks. Eos, 70, 490.
Hewitt, D.A., and Abrecht, J. (1986) Limitations on the interpretation of biotite substitutions from chemical analyses of natural samples. American Mineralogist, 71, 1126–1128.
Holdaway, M.J. (1982) Chemical formulae and activity models for biotite, muscovite, and chlorite applicable to pelitic metamorphic rocks. American Mineralogist, 65, 711–719.
Holdaway, M.J., Guidott, C.V., Novak, J.M., and Henry, W.E. (1982) Polymetamorphism in medium- to high-grade pelitic metamorphic rocks, west-central Maine. Geological Society of America Bulletin, 93, 572–584.
Hounslow, A.W., and Moore, J.M., Jr. (1967) Chemical petrology of Greenville schists near Fernleigh, Ontario. Journal of Petrology, 8, 1–28.
Kohn, M.J., and Spear, F.J. (1989) Realistic propagation of experimental uncertainties in geologic barometry: The "true" story. Eos, 70, 492.
Kretz, R. (1983) Symbols for rock-forming minerals. American Mineralogist, 68, 277–279.
Lee, J.H., and Guggenheim, S. (1981) Single crystal X-ray refinement of pyrophyllite-1Tc. American Mineralogist, 66, 350–357.
Nordstrom, D.K., and Munoz, J.L. (1985) Geochemical thermodynamics, 477 p. Benjamin/Cummings, Menlo Park, California.
Osberg, P.H., Hussey, A.M., II, and Boone, G.M. (1985) Bedrock geologic map of Maine. Department of Conservation, Maine Geological Survey, Augusta, Maine.
Powell, R. (1977) Activity-composition relationships for crystalline solutions. In D.G. Fraser, Ed. Thermodynamics in geology, p. 57–65. Reidel, Boston.
Powell, R. (1978) Equilibrium thermodynamics in petrology: An introduction, 284 p. Harper and Row, New York.
Rebbert, C.R. (1986) Biotite oxidation: An experimental and thermodynamic approach. M.S. thesis, Virginia Polytechnic Institute and State University, Blacksburg, Virginia.
Wang, G.F., and Banno, S. (1987) Non-stoichiometry of interlayer cations in micas from low- to middle-grade metamorphic rocks in the Ryoke and the Sanbagawa belts, Japan. Contributions to Mineralogy and Petrology, 97, 313–319.
White, J.L., and Burns, A.F. (1963) Infra-red spectra of hydronium ion in micaceous minerals. Science, 141, 929–932.
Williams, M.L. (1987) Stratigraphic, structural and metamorphic relationships in Proterozoic rocks from northern New Mexico. Ph.D. thesis, University of New Mexico, Albuquerque, New Mexico.

Manuscript received July 3, 1989
Manuscript accepted November 4, 1990

Appendix 1.

In order to confirm the validity of treating baseline Fe^{3+} in the biotite of Areas A and B as a constant at 8% tetrahedral and 4% octahedral, we examined the data with simple statistics. Grade categories were reduced to five reaction-controlled groups: garnet, staurolite, staurolite + sillimanite, sillimanite, and potassium feldspar + sillimanite in order to average locality and analytical differences. All biotite samples from oxidized and sulfidic assemblages were excluded from this statistical analysis. Averages and standard deviations for $^{[4]}Fe^{3+}$, $^{[6]}Fe^{3+}$, and total Fe^{3+} were computed for each of the five groups of data, both in terms of percentage of total Fe and in formula units. Analytical error on these Mössbauer measurements is ±3% of the total Fe on the percentage figures and ±0.078 for the formula unit data.

Standard deviations (s.d.) in terms of percentages are roughly equal to the known errors owing to precision of the techniques (±3%) as follows:

Zone	$^{[4]}Fe^{3+}$	$^{[6]}Fe^{3+}$	Fe^{3+}_{tot}
Grt	2.5	2.3	2.9
St	1.9	1.7	1.9
St + Sil	1.7	2.6	3.0
Sil	2.8	3.4	3.8
Kfs + Sil	3.2	3.0	1.5
All analyses	2.5	2.8	4.6
Average Fe^{3+} of all analyses	7.8	3.8	11.3
% s.d. of total	32%	74%	41%

Standard deviations in terms of formula units are also similar to the known precision of the technique (±0.078) as follows:

Zone	$^{[4]}Fe^{3+}$	$^{[6]}Fe^{3+}$	Fe^{3+}_{tot}
Grt	0.054	0.065	0.075
St	0.044	0.050	0.056
St + Sil	0.070	0.039	0.077
Sil	0.093	0.065	0.102
Kfs + Sil	0.050	0.103	0.082
All analyses	0.071	0.068	0.123
Average all	0.098	0.200	0.291
% s.d. of total Fe	138%	34%	42%

Standard deviations, in percent of total average, are almost identical either by stoichiometry or as percent of the total Fe except for $^{[6]}Fe^{3+}$, which is poorly defined and has high errors. The grade standard deviations are similar to the overall standard deviations except for total Fe^{3+}. There are no apparent trends in average stoichiometry or percent of Fe by grade. Thus all the variability encountered in our data set can be explained by analytical imprecision.